Journal of Geophysical Research – Solid Earth

Supporting Information for

Elastic Contrast, Rupture Directivity, and Damage Asymmetry in an Anisotropic Bimaterial Strike-Slip Fault at Middle Crustal Depths

Bo Ra Song[1]*, Won Joon Song[1], Scott E. Johnson[1], Christopher C. Gerbi[1], Senthil S. Vel[2]

[1]School of Earth and Climate Sciences, University of Maine, Orono, Maine 04469, USA.
[2]Department of Mechanical Engineering, University of Maine, Orono, Maine 04469, USA.
*Corresponding author: Bo Ra Song (bora.song@maine.edu)

Contents of this file

Figures S1 to S7
Table S1

Additional Supporting Information (File uploaded separately)

Caption for Table S2

Introduction

The supporting information contains a description of the coordinate system used in TESA toolbox (Figure S1), 3D seismic velocities for single crystal of minerals used in the present study (Figure S2), an illustration of polarization of seismic waves (Figure S3), crystallographic orientations of the natural (Figure S4) and synthetic rocks (Figure S5), 2D seismic velocities for single crystal of phlogopite and muscovite (Figure S6), maximum and minimum 2D seismic velocities for the natural and synthetic rocks (Table S1), and an Excel file showing 3D *P*-wave seismic anisotropy and *SH*-wave velocity contrast for natural rocks from the literature (Table S2).

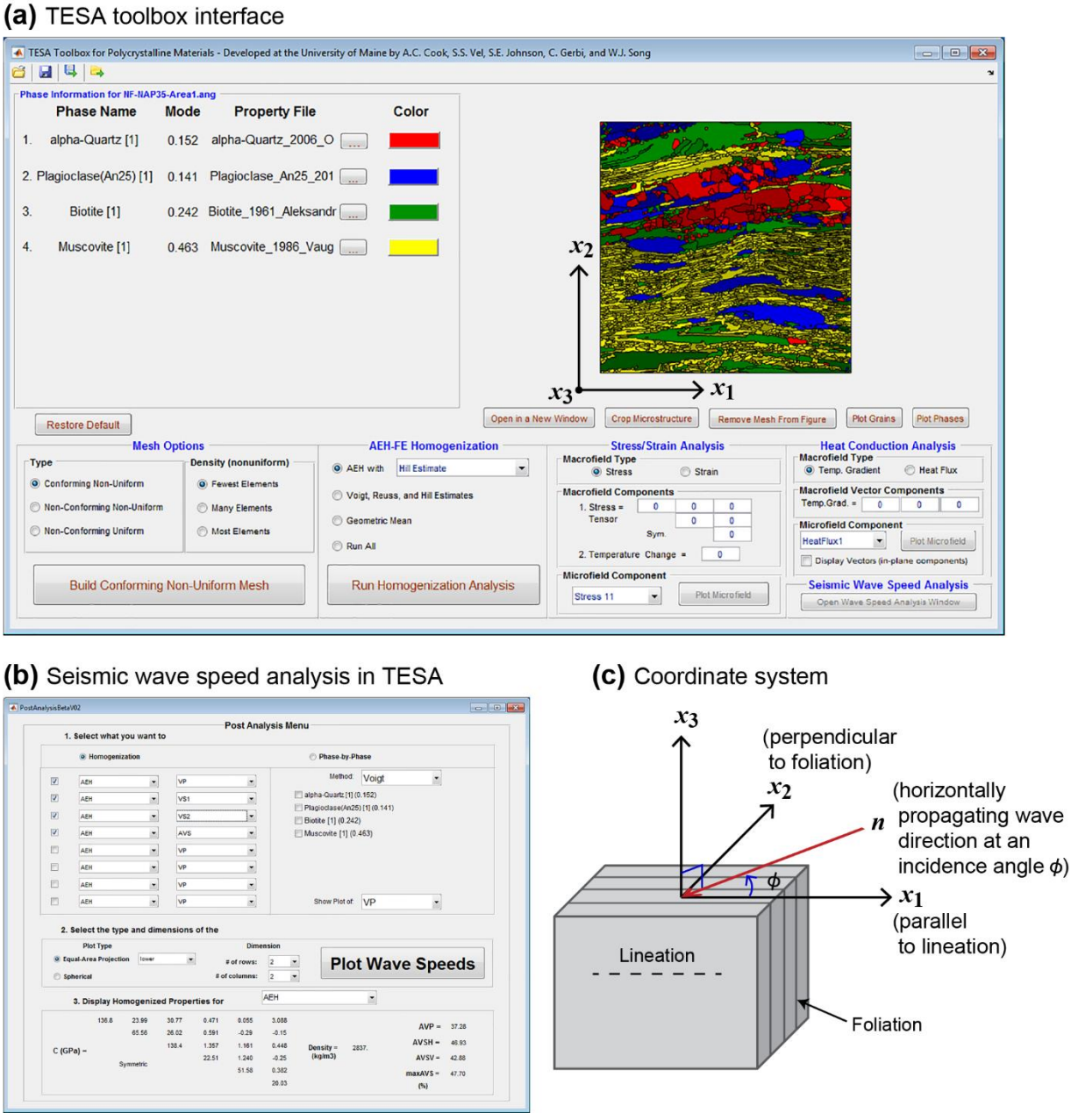

Figure S1. TESA toolbox and reference frame. (a) TESA toolbox interface. Note the reference frame of the *x*1-*x*2-*x*3 axes. (b) Seismic wave speed analysis after computing homogenization elastic properties in TESA. 3D wave speeds can be plotted on equal-area projection or sphere. (c) Coordinate system in TESA and the analyzed samples with vertical foliation and horizontal lineation. This study calculates 2D wave velocities in the *x*1-*x*2 plane as a function of the incidence angle ϕ.

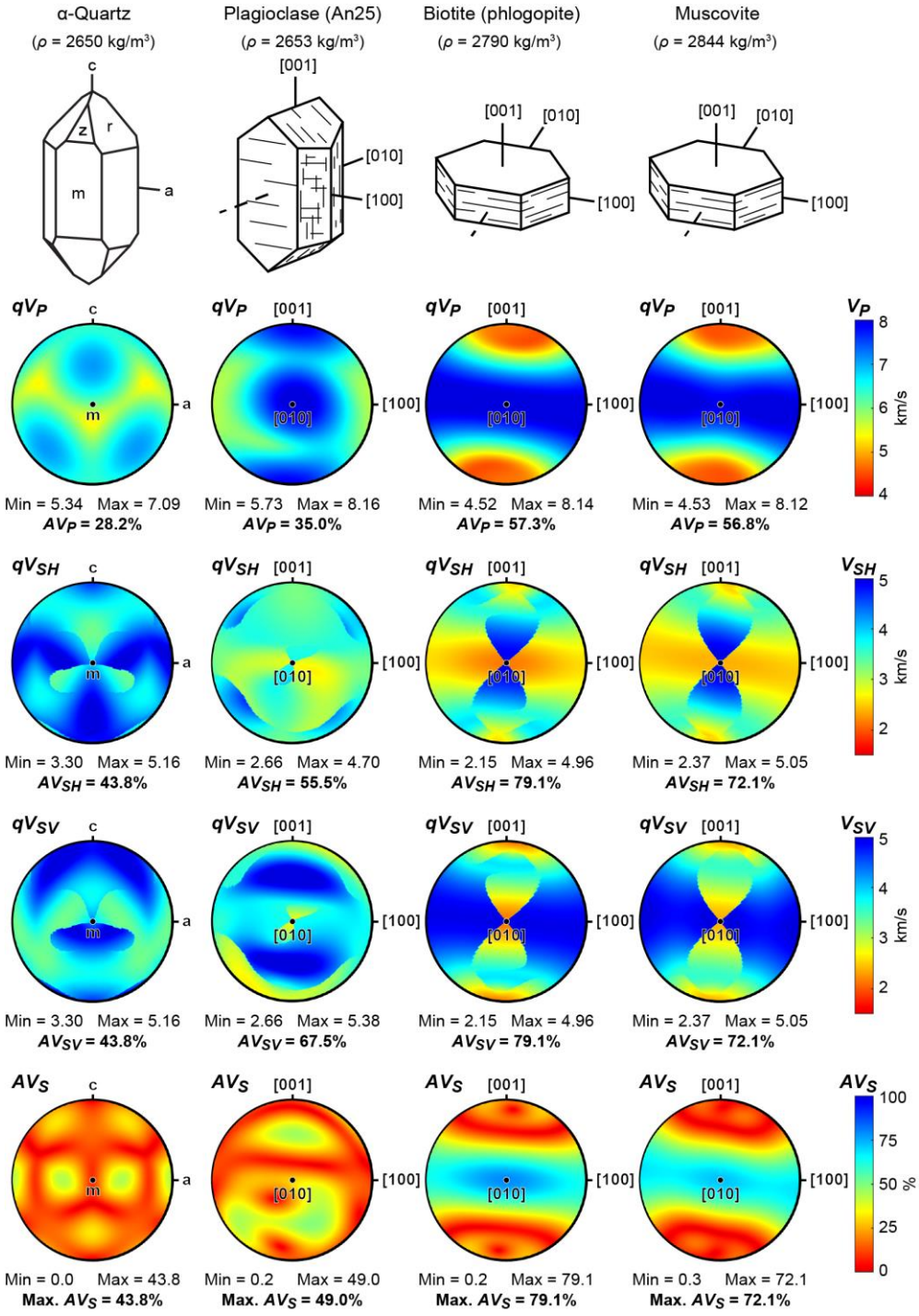

Figure S2. *P*-, *SH*- and *SV*-wave velocities (denoted by qV_P, qV_{SH} and qV_{SV}, respectively) and *S*-wave splitting (AV_S), being plotted in equal-area, upper hemisphere projection, for single crystal of quartz, plagioclase (An25), phlogopite for biotite, and muscovite used in the present study. In this reference frame for single crystal velocities, the horizontal polarization for SH-wave is parallel to the a-c plane in quartz and the [100]-[001] plane in plagioclase, biotite and muscovite. Note that V_{SH} and V_{SV} (and thus their seismic anisotropies) can vary depending on the selected reference frame. 3D velocities of quartz, plagioclase, phlogopite and muscovite show trigonal, triclinic, monoclinic and monoclinic symmetry, respectively, being computed using the elastic properties of Ohno et al. (2006), Brown et al. (2016), Chheda et al. (2014) and Vaughan and Guggenheim (1986), and the densities of 2650, 2653, 2790 and 2844 kg/m^3. Seismic anisotropy (*AV*) for each seismic velocity is calculated from the difference between the maximum and minimum velocities divided by the average of them.

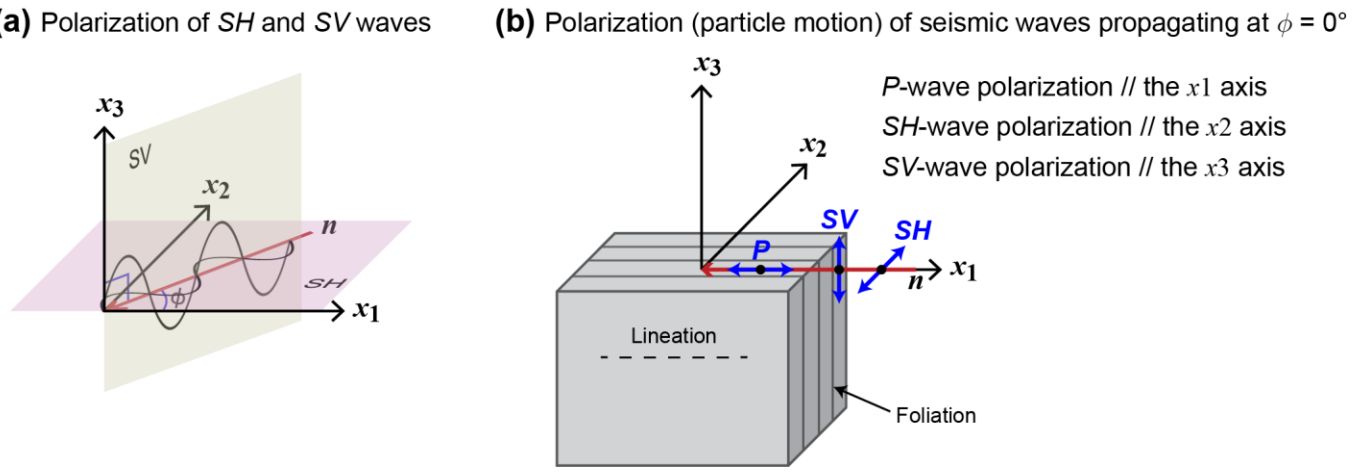

Figure S3. Illustration of polarization of seismic waves. (a) Polarization of the *SH* and *SV* waves horizontally propagating at an incidence angle ϕ. The *SH*-wave polarization is parallel to the *x*1-*x*2 plane. The *SV*-wave polarization direction lies in the planes that are parallel to the *x*3 axis. (b) Particle motion (polarization) of *P*, *SH* and *SV* waves horizontally propagating at $\phi = 0°$ (parallel to the foliation and lineation). The compressional *P* wave has particle motion parallel to the propagation direction (the *x*1 axis). Two shear waves show polarization perpendicular to the propagation direction. The *SH* wave has particle motion parallel to the *x*2 direction (or perpendicular to the foliation). The *SV* wave has particle motion parallel to the *x*3 direction (or perpendicular to the horizontal *x*1-*x*2 plane). ***n***, wave propagation direction.

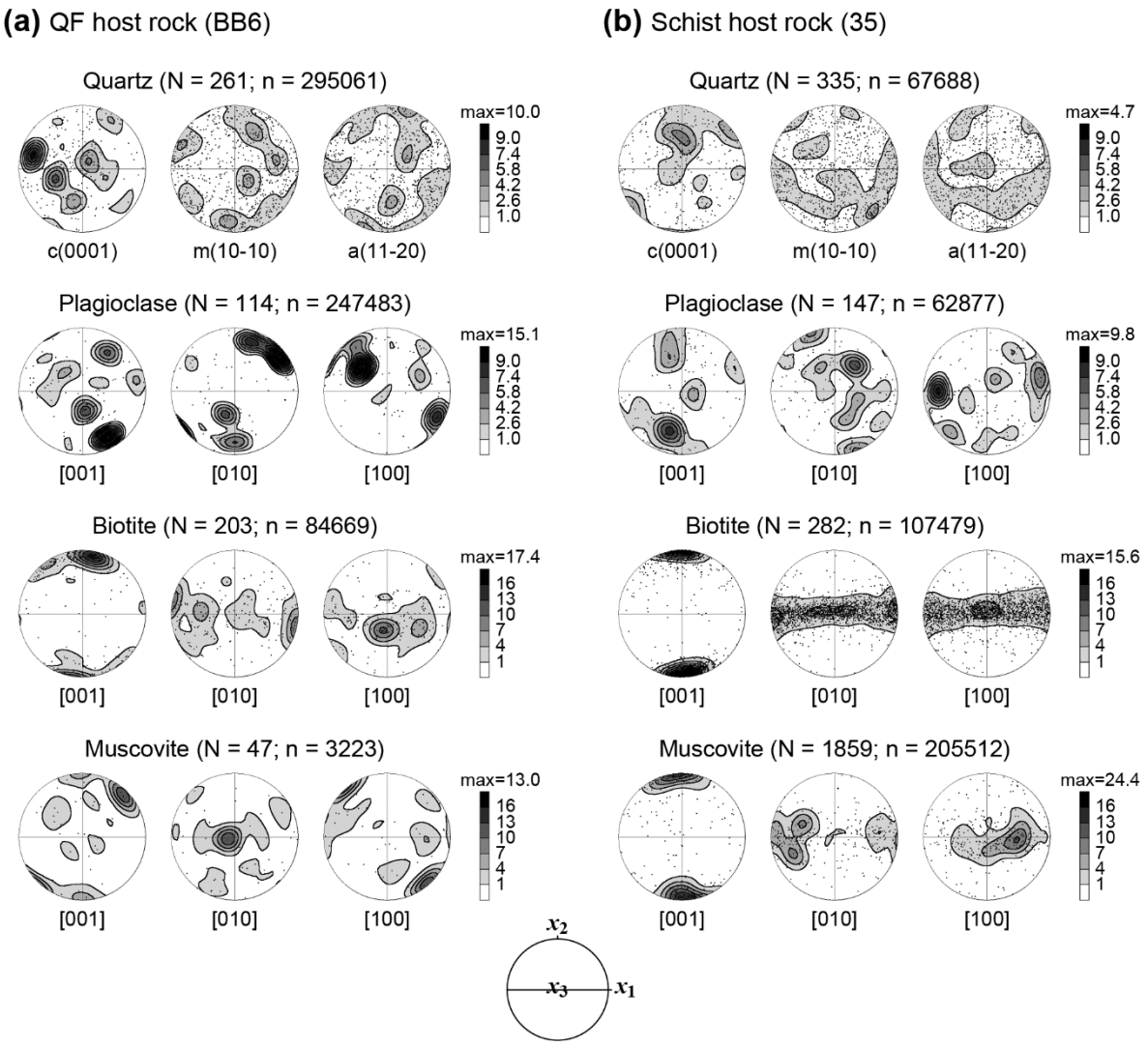

Figure S4. Crystallographic orientations of the natural rocks at all the EBSD analysis points (pixels) plotted in equal-area, upper hemisphere projection (not one-point-per-grain plots) and contoured as multiples of uniform distribution using smoothing parameters with series rank of 10 and Gaussian half-width of 10°. Thus, the contoured pole figures show area-weighted effect, which helps interpret seismic properties of the rocks. (a) Crystallographic orientations of quartz, plagioclase, biotite and muscovite in the QF host rock (sample BB6). (b) Crystallographic orientations of quartz, plagioclase, biotite and muscovite in the schist host rock (sample 35). The reference frame (*x*1-*x*2-*x*3) is displayed in the bottom; the numbers of grains (N) and analysis points (n) are also presented next to each mineral name. Note that the basal (001) planes of biotite and muscovite in the mica-rich schist are strongly parallel to the foliation (the *x*1-*x*3 plane).

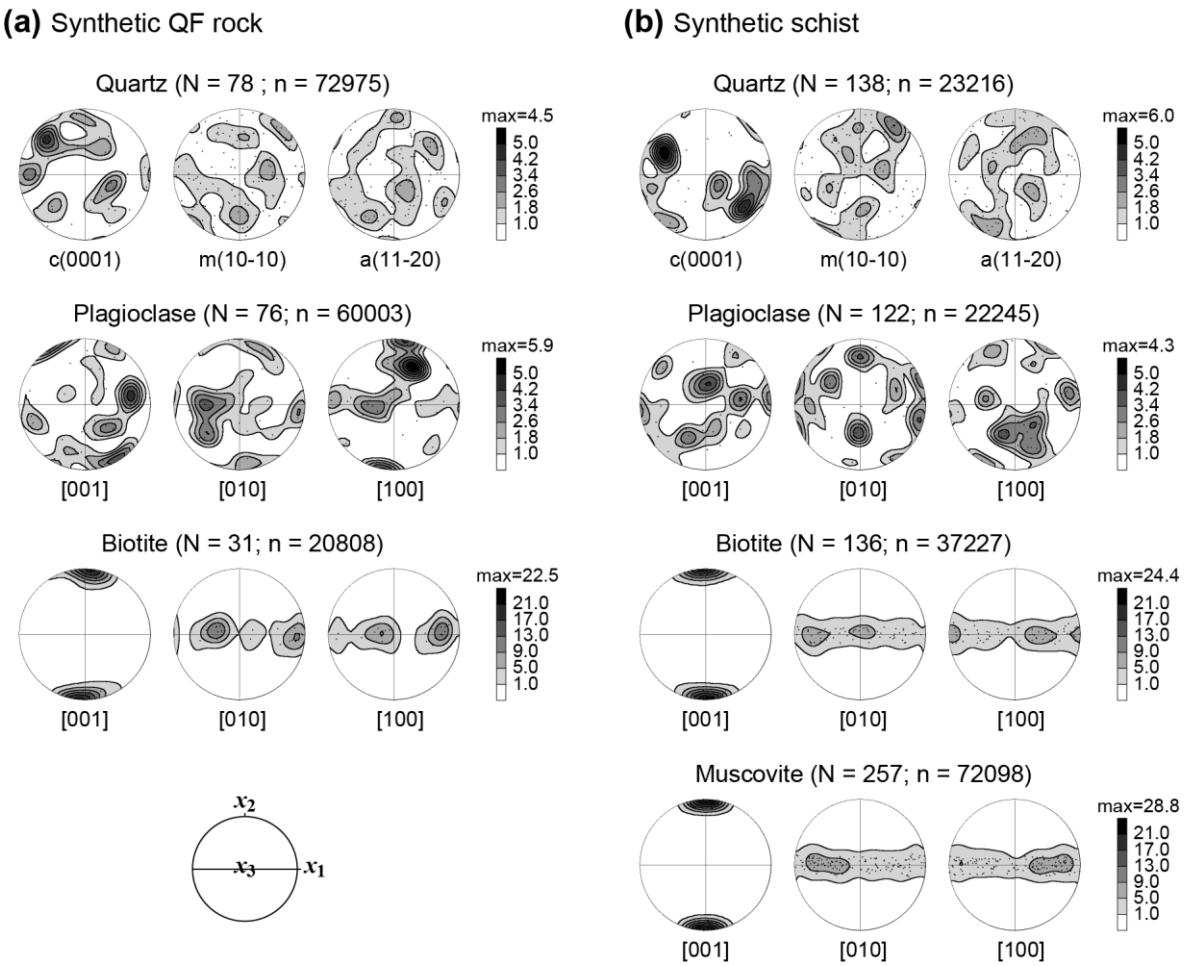

Figure S5. Crystallographic orientations of the synthetic rocks at all the pixels plotted in equal-area, upper hemisphere projection and contoured as multiples of uniform distribution using smoothing parameters with series rank of 10 and Gaussian half-width of 10°. (a) Crystallographic orientations of quartz, plagioclase and biotite in the synthetic QF rock. Muscovite is not plotted because the synthetic QF rock has only one grain of muscovite. (b) Crystallographic orientations of quartz, plagioclase, biotite and muscovite in the synthetic schist. The reference frame (*x*1-*x*2-*x*3) is displayed in the bottom left; the numbers of grains (N) and analysis points (n) are also presented next to each mineral name. Note that the basal (001) planes of micas in both synthetic rocks are strongly parallel to the foliation (the *x*1-*x*3 plane), and the other minerals (quartz and plagioclase) show very weak crystallographic preferred orientations compared to biotite.

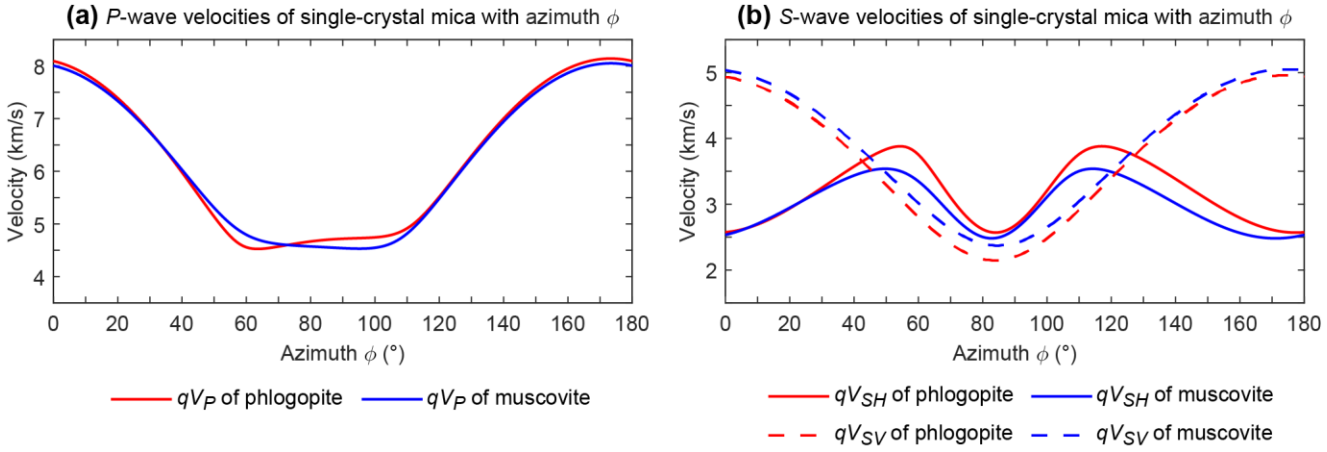

(c) Maximum and minimum seismic velocities of phlogopite and muscovite in (a) and (b)

	P wave		*SH* wave		*SV* wave	
	Max (at ϕ)	Min (at ϕ)	Max (at ϕ)	Min (at ϕ)	Max (at ϕ)	Min (at ϕ)
Phlogopite	8.141 km/s (ϕ = 173°)	4.526 km/s (ϕ = 64°)	3.880 km/s (ϕ = 117°)	2.568 km/s (ϕ = 84°)	4.956 km/s (ϕ = 174°)	2.148 km/s (ϕ = 84°)
			3.880 km/s (ϕ = 54°)[a]	2.569 km/s (ϕ = 177°)[b]		
Muscovite	8.051 km/s (ϕ = 173°)	4.531 km/s (ϕ = 95°)	3.539 km/s (ϕ = 114°)	2.481 km/s (ϕ = 171°)	5.048 km/s (ϕ = 175°)	2.373 km/s (ϕ = 85°)
			3.538 km/s (ϕ = 50°)[a]	2.481 km/s (ϕ = 83°)[b]		

[a]Another ϕ and velocity showing a maximum compared to the surrounding azimuth angles.
[b]Another ϕ and velocity showing a minimum compared to the surrounding azimuth angles.

Figure S6. 2D seismic velocities for single crystals of biotite (phlogopite) and muscovite used in the present study. See Figure S2 for full 3D seismic velocities. (a) *P*-wave velocities (qV_P) of mica in the [100]-[001] plane. (b) *SH*- and *SH*-wave velocities (qV_{SH} and qV_{SV}) of mica in the [100]-[001] plane. If we consider [100] and [001] of mica as *x*1 and *x*2 axes, respectively, then this plot can be viewed as the 2D velocity plots used for rocks with azimuth ϕ from 0° to 180° in the *x*1-*x*2 plane. The 2D seismic velocities in the [100]-[001] plane is not perfectly symmetrical with respect to ϕ = 90° since 3D seismic velocities of phlogopite and muscovite show monoclinic symmetry (Figure S2). (c) Maximum and minimum velocities in (a) and (b) and their azimuth ϕ. *P* wave in both phlogopite and muscovite show a maximum velocity when propagating sub-parallel to the basal (001) plane (ϕ = 173°). The minimum qV_P is present at ϕ = 64° for phlogopite and 95° for muscovite. *SV* wave in phlogopite and muscovite have a minimum velocity at ϕ = 84° and 85°, respectively, due to sub-perpendicular propagation to the basal (001) plane and a maximum velocity at ϕ = 174° or 175°, respectively, because both propagation and polarization directions are sub-parallel to the basal (001) plane. *SH* wave exhibits minimum (or lower) velocities with sub-perpendicular propagation or polarization to the basal (001) plane (ϕ = 84° or 177° for phlogopite; ϕ = 171° or 83° for muscovite). On the other hand, maximum (or higher) qV_{SH} in phlogopite and muscovite is present at an angle where either its propagation or polarization direction is away from the basal (001) plane, and therefore the maximum qV_{SH} in the [100]-[001] plane is much lower than the maximum qV_{SV}.

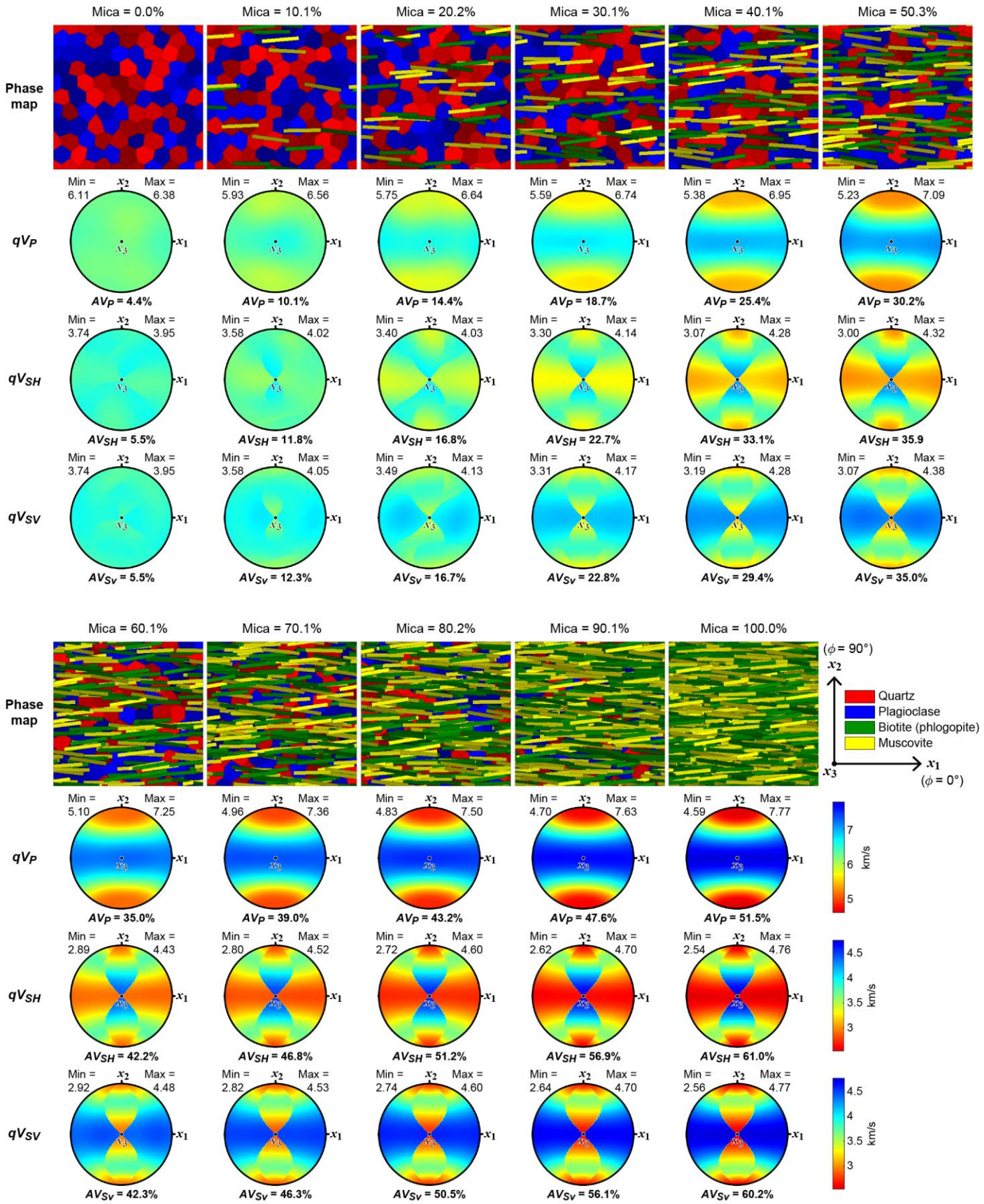
(a) Phase maps and 3D seismic velocities (Bt:Ms = 50:50)
Mica = 0.0%
Mica = 10.1%
Mica = 20.2%
Mica = 30.1%
Mica = 40.1%
Mica = 50.3%
Phase map
qVP
qVSH
qVSV
Min = 6.11 Max = 6.38
AVP = 4.4%
Min = 5.93 Max = 6.56
AVP = 10.1%
Min = 5.75 Max = 6.64
AVP = 14.4%
Min = 5.59 Max = 6.74
AVP = 18.7%
Min = 5.38 Max = 6.95
AVP = 25.4%
Min = 5.23 Max = 7.09
AVP = 30.2%
Min = 3.74 Max = 3.95
AVSH = 5.5%
Min = 3.58 Max = 4.02
AVSH = 11.8%
Min = 3.40 Max = 4.03
AVSH = 16.8%
Min = 3.30 Max = 4.14
AVSH = 22.7%
Min = 3.07 Max = 4.28
AVSH = 33.1%
Min = 3.00 Max = 4.32
AVSH = 35.9
Min = 3.74 Max = 3.95
AVSV = 5.5%
Min = 3.58 Max = 4.05
AVSV = 12.3%
Min = 3.49 Max = 4.13
AVSV = 16.7%
Min = 3.31 Max = 4.17
AVSV = 22.8%
Min = 3.19 Max = 4.28
AVSV = 29.4%
Min = 3.07 Max = 4.38
AVSV = 35.0%
Mica = 60.1%
Mica = 70.1%
Mica = 80.2%
Mica = 90.1%
Mica = 100.0%
(ϕ = 90°)
(ϕ = 0°)
Quartz
Plagioclase
Biotite (phlogopite)
Muscovite
Min = 5.10 Max = 7.25
AVP = 35.0%
Min = 4.96 Max = 7.36
AVP = 39.0%
Min = 4.83 Max = 7.50
AVP = 43.2%
Min = 4.70 Max = 7.63
AVP = 47.6%
Min = 4.59 Max = 7.77
AVP = 51.5%
7
6
5
km/s
Min = 2.89 Max = 4.43
AVSH = 42.2%
Min = 2.80 Max = 4.52
AVSH = 46.8%
Min = 2.72 Max = 4.60
AVSH = 51.2%
Min = 2.62 Max = 4.70
AVSH = 56.9%
Min = 2.54 Max = 4.76
AVSH = 61.0%
4.5
4
3.5
3
km/s
Min = 2.92 Max = 4.48
AVSV = 42.3%
Min = 2.82 Max = 4.53
AVSV = 46.3%
Min = 2.74 Max = 4.60
AVSV = 50.5%
Min = 2.64 Max = 4.70
AVSV = 56.1%
Min = 2.56 Max = 4.77
AVSV = 60.2%
4.5
4
3.5
3
km/s

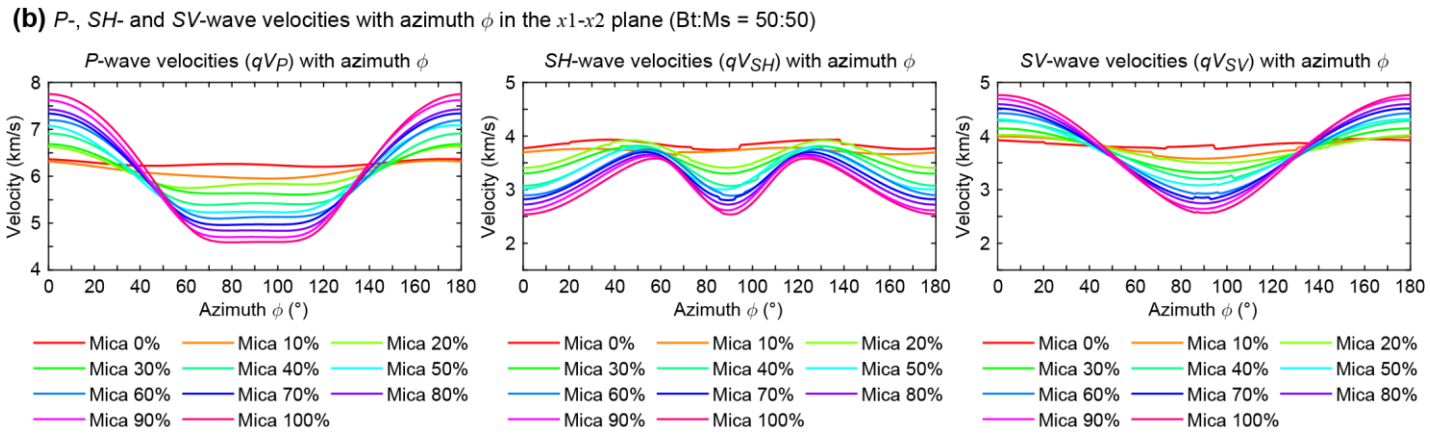

Figure S7. Effect of mica content, in synthetic rocks, on seismic velocities. (a) Phase maps and 3D seismic velocities of synthetic microstructures with mica contents from 0% to 100% in 10% intervals. Each phase map with mica has the same ratio of biotite and muscovite (Bt:Ms = 50:50). The coordinate system and phase color information are shown next to the phase map with 100% mica. *P*-wave (qV_P) and two *S*-wave velocities (qV_{SH} and qV_{SV}) are presented in equal-area, upper hemisphere projection and with the same color limits for comparison. **S**eismic anisotropy (AV_P, AV_{SH} and AV_{SV}, respectively) for qV_P, qV_{SH} and qV_{SV} of each case is also displayed below each 3D seismic velocity plot. (b) 2D seismic velocities of *P*, *SH* and *SV* waves for each synthetic microstructure in (a) plotted with azimuth ϕ from 0° to 180° in the *x*1-*x*2 plane.

Table S1

Maximum and Minimum Seismic Velocities and their Differences for the Natural and Synthetic Rocks in the x*1-*x*2 Plane*

	Seismic velocity [km/s]								
	P wave			*SH* wave			*SV* wave		
Rock sample	Max (at ϕ[a])	Min (at ϕ)	Diff[b]	Max (at ϕ)	Min (at ϕ)	Diff	Max (at ϕ)	Min (at ϕ)	Diff
Natural QF[c] (BB6)	6.408 (ϕ = 19°)	5.838 (ϕ = 82°)	0.570	3.971 (ϕ = 76°)	3.505 (ϕ = 25°)	0.467	3.964 (ϕ = 153°)	3.562 (ϕ = 87°)	0.403
Natural Schist (35)	7.124 (ϕ = 3°)	4.980 (ϕ = 96°)	2.144	3.598 (ϕ = 130°)	2.859 (ϕ = 3°)	0.739	4.397 (ϕ = 3°)	3.004 (ϕ = 93°)	1.393
Synthetic QF	6.488 (ϕ = 174°)	5.863 (ϕ = 56°)	0.625	3.924 (ϕ = 42°)	3.515 (ϕ = 174°)	0.409	4.095 (ϕ = 177°)	3.570 (ϕ = 97°)	0.525
Synthetic Schist	7.413 (ϕ = 0° or 180°)	4.918 (ϕ = 81°)	2.495	3.663 (ϕ = 55°)	2.798 (ϕ = 90°)	0.865	4.514 (ϕ = 0° or 180°)	2.827 (ϕ = 95°)	1.687

Note: 2D seismic velocities at all azimuth ϕ for the natural and synthetic rocks are plotted in Figures 4 and 5, respectively.

[a]Azimuth ϕ is the incidence angle of waves with respect to the x1 direction in the horizontal x1-x2 plane. For example, the *x*1 and *x*2 directions are ϕ = 0° and 90°, respectively. See Figure S1c for the coordinate system.

[b]Difference (Diff) = maximum velocity − minimum velocity.

[c]QF = quartzofeldspathic rock.

Table S2

Comparison with the literature for qV_P seismic anisotropy and qV_{SH} contrast relative to the SCSZ QF rock (BB6) at $\phi = 0°$

Table S2

Comparison with the literature for VP seismic anisotropy and VSH contrast relative to the SCSZ QF rock (BB6) at ϕ = 0°

Category	Lithology	Sample	Reference	Method	Quartz modal%	Feldspar modal%	**Mica modal %**	Subtotal modal% for major phases	Selected Pc for linear regression (MPa)	[X] VP0 at 0 MPa (km s^{-1})	[X] dVP/dP (10^{-4} km s^{-1} MP^{-1})	[Y] VP0 at 0 MPa (km s^{-1})	[Y] dVP/dP (10^{-4} km s^{-1} MP^{-1})	[Z] VP0 at 0 MPa (km s^{-1})	[Z] dVP/dP (10^{-4} km s^{-1} MP^{-1})	**Seismic anisotropy of VP0 at 0 MPa (%)**	[SH // x1] VS0 (km/s) at 0 Mpa	[SH // x1] dVS/dP-XZ (10^{-4} km s^{-1} MP^{-1})	**VSH contrast relative to SCSZ QF at ϕ = 0° (%)**	More compliant than SCSZ QF?
This study	QF rock	BB6	This study	EBSD	46.80	39.26	**13.94**	100								**15.32**	3.6983		**0.00**	
This study	Schist	35	This study	EBSD	15.26	14.18	**70.56**	100								**37.88**	2.6512		**32.98**	Yes
Quartzite	Quartzite (metapsammite)	IV-91	Burlini & Fountain (1993)	Petrophysical	74.21	7.89	**17.76**	99.86	250	5.76	4.11	6.15	4.04	6.26	2.73	**8.32**	3.41	1.49	**8.11**	Yes
Quartzite	Quartzite (metapsammite)	IV-92	Burlini & Fountain (1993)	Petrophysical	70.06	6.51	**22.93**	99.5	250	5.57	5.43	6.41	2.93	6.45	2.54	**14.64**				
Quartzite	Quartzite (metapsammite)	IV-93	Burlini & Fountain (1993)	Petrophysical	68.84	22.9	**7.79**	99.53	250	5.95	3.18	6.73	4.84	6.48	3.51	**12.30**				
Quartzite	Quartzite (metasandstone)	664-2	Kastner et al. (2021)	Petrophysical	72	19	**3**	94	100	6.09		6.31		6.04		**4.37**				
Quartzite	Quartzite (metasandstone)	664-2	Kastner et al. (2021)	EBSD	72	19	**3**	94								**5.76**				
Igneous rock	Granite	Westerly	Birch (1960)	Petrophysical	27.5	66.8	**4.5**	98.8	400	6.0929	2.6071	6.0357	1.9643	5.9257	1.9643	**2.78**				
Igneous rock	Granite	Stone Mt	Birch (1960)	Petrophysical	26	70	**4**	100	400	6.2571	1.6429	6.1543	2.7857	6.18	1.75	**1.66**				
Igneous rock	Granite	Chelmsford	Birch (1960)	Petrophysical	31	62	**5**	98	400	6.2043	1.7857	6.1529	2.1071	6.0715	2.4286	**2.16**				
Igneous rock	Quartz monzonite	Porterville	Birch (1960)	Petrophysical	34	60	**4**	98	400	6.1729	2.1071	6.1157	2.9643	6.09	2.25	**1.35**				
Igneous rock	Granite	Barre	Birch (1960)	Petrophysical	26	62	**12**	100	400	6.2086	2.0714	6.1814	2.4286	6.1271	2.1429	**1.32**				
Igneous rock	Granite	Sacred Heart	Birch (1960)	Petrophysical	26	68	**3**	97	400	6.3414	1.6786	6.3086	1.8214	6.1457	1.9643	**3.13**				
Igneous rock	Granodiorite	Butt	Birch (1960)	Petrophysical	27	63	**7**	97	400	6.3986	1.8214	6.3157	2.4643	6.3143	2.2857	**1.33**				
Igneous rock	Granite	IV-44	Burke & Fountain (1990)	Petrophysical	45	48	**7**	100	300	6.368	2.6	6.2	3	6.123	3.6	**3.92**				
Igneous rock	Tonalite	L26	Chroston & Brooks (1989)	Petrophysical	21	59	**20**	100	200	5.9983	10.5	6.3117	3.5	5.9783	2.5	**5.43**				
Igneous rock	Tonalite	L27	Chroston & Brooks (1989)	Petrophysical	12	46	**41**	99	200	6.2583	4.5	6.26	2	5.83	8	**7.11**				
Igneous rock	Tonalite/Diorite	H5	Chroston & Brooks (1989)	Petrophysical	18	48	**26**	92	200	6.0483	9.5	6.13	5	5.905	2.5	**3.74**				
Igneous rock	Granodiorite	H7	Chroston & Brooks (1989)	Petrophysical	30	30	**40**	100	200	6.275	6.5	6.0817	9.5	5.7517	7.5	**8.70**				
Igneous rock	Granite	H18	Chroston & Brooks (1989)	Petrophysical	44	48	**4**	96	200	6.2	5	5.9767	7	6.0067	6	**3.67**				
Igneous rock	Tonalite	KZ-35	Fountain et al. (1990)	Petrophysical	29.5	69	**0**	98.5	200	6.2333	3	6.4133	2.5	6.3267	2.5	**2.85**				
Igneous rock	Tonalite	ai117	Hurich et al. (2001)	Petrophysical	41	53.7	**0**	94.7	200	6.1016	1.75	6	2.75	5.9533	2.5	**2.46**				
Igneous rock	Granite	D95-13	Kern et al. (1999)	Petrophysical	20	77	**3**	100	200	5.8467	3.5	5.8767	3.5	5.7933	5.5	**1.43**				
Igneous rock	Granite	S11-S12	Khazanehdari et al. (2000)	Petrophysical	38	42	**19**	99	300	5.658	3.63	6.485	2.07	6.049	4.04	**13.62**				
Igneous rock	Granite	S53,S92-S98	Khazanehdari et al. (2000)	Petrophysical	50	44	**6**	100	300	5.918	9.85	5.947	8.3	5.958	8.4	**0.67**				
Igneous rock	Granite	B-9	Long (1994)	Petrophysical	43.9	51.1	**4.4**	99.4	200	6	2	6.22	2.5	6.2267	2.25	**3.71**				
Igneous rock	Granite	B-10	Long (1994)	Petrophysical	20.5	72.5	**5.9**	98.9	200	6.2	2	6.2833	0.75	6.15	2.25	**2.14**				
Igneous rock	Granite	B-18	Long (1994)	Petrophysical	38.4	60.1	**1.2**	99.7	200	6.1233	0.75	6.08	2.5	6.0867	2.25	**0.71**				
Igneous rock	Granite	B-24	Long (1994)	Petrophysical	81.3	6.6	**10.2**	98.1	200	6.0067	2.25	6.24	2.25	5.78	2	**7.65**				
Igneous rock	Granite	B-28	Long (1994)	Petrophysical	31.4	63.4	**2.5**	97.3	200	6.2533	2	6.2167	3.5	6.4733	2	**4.04**				
Igneous rock	Granite	B-33	Long (1994)	Petrophysical	50.8	43	**3.5**	97.3	200	6.02	2.5	6.0867	2.75	6.2633	2	**3.96**				
Igneous rock	Granite	B-43	Long (1994)	Petrophysical	40.8	57	**0.4**	98.2	200	6.12	2.5	6.25	2.5	6.2167	1.75	**2.10**				
Igneous rock	Granite	B-46	Long (1994)	Petrophysical	20.7	64.9	**9.3**	94.9	200	6.1467	2.25	6.0167	2.25	6.1567	1.75	**2.30**				
Igneous rock	Granite	B-49	Long (1994)	Petrophysical	30	67.6	**1.6**	99.2	200	6.0867	1.25	5.9467	1.75	6.1233	2.25	**2.93**				
Igneous rock	Granite	B-58	Long (1994)	Petrophysical	20.3	74.4	**4.4**	99.1	200	5.7533	4.75	6.0433	4.75	5.8667	5	**4.92**				
Igneous rock	Granite	B-60	Long (1994)	Petrophysical	25.4	73.3	**0.9**	99.6	200	6.12	1.75	6.1833	3.5	6.0733	3	**1.79**				
Igneous rock	Granite	B-61	Long (1994)	Petrophysical	25.6	62.9	**4.9**	93.4	200	6.1233	2.5	6.0933	2.5	6.0833	3	**0.66**				
Igneous rock	Granite	B-66	Long (1994)	Petrophysical	20.2	69.3	**6.6**	96.1	200	5.9767	3.5	6.1767	3	6.1967	3	**3.61**				
Schist	Schist (metapelite)	IV-83	Burlini & Fountain (1993)	Petrophysical	24.54	32.77	**42.14**	99.45	250	5.38	5.17	6.3	6.31	6.38	2.18	**17.01**	2.89	3.24	**24.54**	Yes
Schist	Schist (metapelite)	IV-85	Burlini & Fountain (1993)	Petrophysical	48.88	15.12	**34.48**	98.48	250	5.61	5	6.52	5.51	6.47	3.4	**15.00**	3.15	3.65	**16.01**	Yes
Schist	Schist (metapelite)	IV-86	Burlini & Fountain (1993)	Petrophysical	49.19	12.64	**37.06**	98.89	250	5.47	5.54	6.32	3.92	6.13	4.7	**14.42**				
Schist	Schist (metapelite)	IV-87	Burlini & Fountain (1993)	Petrophysical	42.52	23.83	**31.91**	98.26	250	5.65	5.1	6.58	3.43	6.26	4.41	**15.21**	3.53	2.54	**4.66**	Yes
Schist	Schist (metapelite)	IV-88	Burlini & Fountain (1993)	Petrophysical	31.03	3.46	**65.06**	99.55	250	5.42	6.86	7.12	5.48	6.91	4.01	**27.11**				
Schist	Schist (metapelite)	IV-90	Burlini & Fountain (1993)	Petrophysical	39.05	17.06	**42.89**	99	250	5.26	6.79	6.75	4.11	6.54	3.37	**24.81**	3.25	1.24	**12.90**	Yes
Schist	Mica schist	S8	Chroston & Brooks (1989)	Petrophysical	50	0	**50**	100	100	6.7	0	6.56	3	5.4967	10.5	**19.73**				
Schist	Schist (Haast)	A-1	Godfrey et al. (2000)	Petrophysical	65	7	**25**	97	200	5.7223	1.605	6.5147	1.085	6.4512	0.96	**12.95**	3.1962	0.62	**14.57**	Yes
Schist	Schist (Haast)	A-5	Godfrey et al. (2000)	Petrophysical	25	17	**54**	91	200	5.5559	2.295	6.5054	0.65	6.1521	0.625	**15.74**	2.8019	0.905	**27.58**	Yes
Schist	Schist (Haast)	A-12	Godfrey et al. (2000)	Petrophysical	25	37	**35**	97	200	5.8348	1.74	6.5182	1.05	6.2579	1.445	**11.06**	2.9167	0.585	**23.63**	Yes
Schist	Schist (Haast)	A-13	Godfrey et al. (2000)	Petrophysical	55	6	**32**	93	200	5.8447	1.385	6.5555	0.925	7.0246	0.61	**18.34**	3.3742	0.44	**9.17**	Yes
Schist	Schist (Haast)	A-18	Godfrey et al. (2000)	Petrophysical	50	16	**30**	96	200	5.8048	2.6	6.4707	1.515	6.7106	1.31	**14.47**	3.2978	0.96	**11.45**	Yes
Schist	Schist (Haast)	A-33	Godfrey et al. (2000)	Petrophysical	54	20	**20**	94	200	5.9061	2.765	6.2852	1.56	6.1781	1.715	**6.22**	3.4682	0.81	**6.42**	Yes
Schist	Schist (Haast)	A-35	Godfrey et al. (2000)	Petrophysical	49	7	**42**	98	200	5.77	1.83	6.8128	1.01	6.2765	1.275	**16.58**	3.483	0.46	**6.00**	Yes
Schist	Schist (Haast)	A-43	Godfrey et al. (2000)	Petrophysical	42	48	**4**	94	200	6.148	1.32	6.943	0.84	6.9435	0.835	**12.15**	3.6211	0.285	**2.11**	Yes
Schist	Schist (Coldfoot)	TA-80	Godfrey et al. (2000)	Petrophysical	38	16	**42**	96	200	5.7656	1.97	6.3305	1.125	6.3472	0.86	**9.60**	3.1455	0.525	**16.16**	Yes
Schist	Schist	GLG119	Ji et al. (2015)	EBSD	33	46	**20**	99								**11.10**				
Schist	Schist	GLG132J	Ji et al. (2015)	EBSD	60	14	**26**	100								**16.40**				
Schist	Qtz-Bt schist	GLG257	Ji et al. (2015)	EBSD	60	0	**40**	100								**25.50**				
Schist	Qtz-Bt schist	GLG258	Ji et al. (2015)	Petrophysical	55	0	**45**	100	200	6.2898	2.4667	6.0292	3.4267	5.0025	3.47	**22.80**	2.9687	3.15	**21.89**	Yes
Schist	Qtz-Bt schist	GLG258	Ji et al. (2015)	EBSD	55	0	**45**	100								**25.40**				
Schist	Qtz-Bt-Ms schist	YN1389	Ji et al. (2015)	EBSD	67	0	**32**	99								**22.20**				
Schist	Pl-Bt schist	YK21A	Ji et al. (2015)	Petrophysical	6	39	**47**	92	200	6.0978	1.76	5.9608	2.49	5.6052	2.1	**8.42**	3.1656	1.5	**15.52**	Yes
Schist	Qtz-Bt schist	P5	Ji et al. (2015)	Petrophysical	75	0	**22**	97	200	6.42	3.2533	6.1668	3.5	5.7635	4.2467	**10.78**				
Schist	Qtz-Bt schist	S382	Ji et al. (2015)	Petrophysical	80	0	**18**	98	200	6.17	3.2533	6.023	3	5.6702	3.5	**8.44**				
Schist	Qtz-Bt schist	S19	Ji et al. (2015)	Petrophysical	62	13	**25**	100	200	6.396	2.7567	5.9291	1.5	5.6591	2.5	**12.23**				
Schist	Qtz-Fsp-Bt schist	S3530	Ji et al. (2015)	Petrophysical	40	49	**11**	100	200	7.0335	2.2467	6.4168	2.2467	5.8532	2.7533	**18.32**				
Schist	Qtz-Fsp-Bt schist	S1132.1	Ji et al. (2015)	Petrophysical	35	37	**28**	100	200	5.976	2.7567	5.876	2.7567	5.2791	3.5	**12.38**				
Schist	Mica schist	569-2	Kastner et al. (2021)	Petrophysical	2	12	**75**	89	100	6.67		6.36		5.5		**19.23**				
Schist	Mica schist	569-2	Kastner et al. (2021)	EBSD	2	12	**75**	89								**14.61**				
Schist	Mica schist	651-5	Kastner et al. (2021)	Petrophysical	10	26	**54**	90	100	6.74		6.41		5.64		**17.77**				
Schist	Grt-Bt-Sill schist (kinzigite)	S45	Khazanehdari et al. (2000)	Petrophysical	35	34	**22**	91	300	6.476	4.46	6.715	5.83	6.58	4.37	**3.62**				
Schist	Schist	Sample A (planar)	Naus-Thijssen et al. (2011)	EBSD	30.4	13.1	**56.5**	100								**31.37**	2.9910		**21.15**	Yes
Schist	Felsic schist	CD01	Watling (2017)	EBSD	32.3	21.7	**40.4**	94.4								**19.42**				
Schist	Mafic schist	CD05	Watling (2017)	EBSD	31.2	6.5	**59.5**	97.2								**25.13**				
Schist	Felsic schist	CD09	Watling (2017)	EBSD	31.3	10.3	**54.4**	96								**19.42**				
Schist	Felsic schist	CD14	Watling (2017)	EBSD	33.8	14.5	**50.6**	98.9								**19.19**				
Gneiss	Granodioritic gneiss	Bethlehem	Birch (1960)	Petrophysical	20	60	**18**	98	400	6.2229	2.1071	6.0486	2.5714	5.9129	2.6071	**5.11**				
Gneiss	Orthogneiss	GFTZ-26	Burke (1991)	Petrophysical	20	67.2	**10.9**	98.1	300	6.082	1.9	6.329	2.3	6.103	4.1	**3.98**				
Gneiss	Paragneiss	GFTZ-30	Burke (1991)	Petrophysical	30.1	32.6	**35.1**	97.8	300	5.833	0.6	6.669	2.3	6.368	1.6	**13.37**				
Gneiss	Paragneiss	GFTZ-41	Burke (1991)	Petrophysical	31.1	40.7	**22.7**	94.5	300	6.046	0.7	6.394	1.3	6.334	1.3	**5.59**				
Gneiss	Paragneiss	GFTZ-49	Burke (1991)	Petrophysical	65.8	24.1	**9.2**	99.1	300	5.974	1.3	6.041	0.7	6.321	0.7	**5.64**				
Gneiss	Paragneiss	GFTZ-55	Burke (1991)	Petrophysical	23.9	37.5	**36.7**	98.1	300	6.001	0.7	5.952	2.4	6.181	1.7	**3.77**				
Gneiss	Orthogneiss	GFTZ-82	Burke (1991)	Petrophysical	30	55.4	**8.6**	94	300	6.198	1.6	6.298	1.6	6.354	1.3	**2.49**				
Gneiss	Paragneiss	GFTZ-91	Burke (1991)	Petrophysical	26.7	42.5	**23.7**	92.9	300	6.116	1.7	6.517	0.9	6.274	1.3	**6.35**				
Gneiss	Orthogneiss	IV-33	Burke & Fountain (1990)	Petrophysical	51	31	**18**	100	300	5.813	6.6	5.983	4.6	6.028	4.6	**3.63**				
Gneiss	Paragneiss	IV-37	Burke & Fountain (1990)	Petrophysical	74	6	**20**	100	300	5.766	3.7	6.238	2.6	5.993	3.6	**7.86**				
Gneiss	Paragneiss	IV-43	Burke & Fountain (1990)	Petrophysical	55	3	**41**	99	300	5.562	4.9	5.943	2.6	5.915	5	**6.62**				
Gneiss	Paragneiss	IV-52	Burke & Fountain (1990)	Petrophysical	62	5	**30**	97	300	6.065	4	6.436	3.7	6.542	2.9	**7.57**				
Gneiss	Paragneiss	IV-53	Burke & Fountain (1990)	Petrophysical	51	13	**33**	97	300	5.715	3	6.199	4.3	6.061	3.7	**8.12**				
Gneiss	Orthogneiss	IV-55	Burke & Fountain (1990)	Petrophysical	67	16	**17**	100	300	5.68	5	5.853	5.6	5.813	5.6	**3.00**				
Gneiss	Tonalitic gneiss	KZ-5	Fountain et al. (1990)	Petrophysical	27.3	60.4	**8.1**	95.8	200	6.3933	3.75	6.4533	3.5	6.43	3.6	**0.93**				
Gneiss	Tonalitic gneiss	KZ-4	Fountain et al. (1990); Salisbury & Fountain (1994)	Petrophysical	33.2	56.6	**8.2**	98	200	6.2467	3.25	6.4333	2.5	6.3967	2.75	**2.94**	3.79	0.5	**2.45**	No
Gneiss	Quartz diorite gneiss	KZ-38b	Fountain et al. (1990); Salisbury & Fountain (1994)	Petrophysical	16.5	77	**5**	98.5	200	6.26	2.25	6.43	2.75	6.4367	3.25	**2.78**	3.667	1.25	**0.85**	Yes
Gneiss	Bt-Ms-Pl-Kfs orthogneiss	B1578R14P18t	Ji et al. (2007)	Petrophysical	25	65	**7**	97	400	6.452	1.855			5.944	1.527	**8.20**				
Gneiss	Bt-Hbl-Pl-Kfs paragneiss	B2184R88P4s	Ji et al. (2007)	Petrophysical	40	55	**4**	99	400	5.954	1.739			6.17	1.264	**3.56**				
Gneiss	Granitic gneiss	GLG14	Ji et al. (2015)	Petrophysical	28	68	**3.7**	99.7	200	5.5145	3.13	5.5205	3.87	5.3065	3.8467	**3.95**	3.2984	3.0133	**11.43**	Yes
Gneiss	Granitic gneiss	GLG97-2	Ji et al. (2015)	Petrophysical	34	64	**1.8**	99.8	200	5.4946	3.25	5.3948	4.5233	5.4426	3.9467	**1.83**	3.3506	2.05	**9.87**	Yes
Gneiss	Dioritic gneiss	GLG134	Ji et al. (2015)	EBSD	20	50	**30**	100								**16.30**				
Gneiss	Paragneiss	593-4	Kastner et al. (2021)	Petrophysical	31	13	**45**	89	100	6.9		6.52		5.08		**30.38**				
Gneiss	Paragneiss	593-4	Kastner et al. (2021)	EBSD	31	13	**45**	89								**9.54**				
Gneiss	Tonalitic gneiss	D95-16	Kern et al. (1999)	Petrophysical	13	71	**12**	96	200	6.0533	3.75	6.0333	4.75	5.9	6.25	**2.56**				
Gneiss	Trondhjemitic gneiss	D95-44	Kern et al. (1999)	Petrophysical	55	27	**12**	94	200	6.32	4	6.1467	4	5.8167	5.75	**8.29**				
Gneiss	Bt gneiss	38098S	Kern et al. (2001)	Petrophysical	23	47	**30**	100	200	6.13	10.5	6.07	7.25	5.3167	8.25	**14.21**				
Gneiss	Bt-Pl gneiss	PP358	Kern et al. (2001)	Petrophysical	32	43	**23**	98	200	6.53	1	6.06	1.75	5.8267	3.5	**11.38**				
Gneiss	Bt-Pl gneiss	PP363	Kern et al. (2001)	Petrophysical	26	49	**23**	98	200	6.4667	2	6.24	2	5.63	3.75	**13.83**				
Gneiss	Gneiss (previously known as schist)	OKU-578	Kern et al. (2009)	Petrophysical	34.1	19.9	**45.1**	99.1	200	6.748	1.7	5.972	2.7	5.012	6.4	**29.52**				
Gneiss	Gneiss (previously known as schist)	OKU-676	Kern et al. (2009)	Petrophysical	42.3	37	**19.8**	99.1	200	6.47	1	6.22	1	5.536	3	**15.56**	3.282		**11.93**	Yes
Gneiss	Gneiss (previously known as schist)	OKU-1093	Kern et al. (2009)	Petrophysical	29.2	39	**31.7**	99.9	200	6.588	1.8	5.97	3.5	5.504	3.9	**17.93**				
Gneiss	Gneiss (previously known as schist)	OKU-1844	Kern et al. (2009)	Petrophysical	36.6	38.1	**24.4**	99.1	200	6.566	1.2	6.256	1.7	5.28	6.3	**21.71**				
Gneiss	Gneiss (previously known as schist)	OKU-818	Kern et al. (2008,2009)	Petrophysical	39.9	37.4	**22.6**	99.9	200	6.47	1.4	5.886	2	5.512	4.2	**15.99**	3.778		**2.13**	No
Gneiss	Gneiss	S59	Khazanehdari et al. (2000)	Petrophysical	31	25	**39**	95	300	5.587	5.83	5.956	3.53	5.984	3.37	**6.86**				
Gneiss	Orthogneiss	S123	Khazanehdari et al. (2000)	Petrophysical	45	45	**10**	100	300	5.723	3.73	5.999	4.15	5.99	4.1	**4.71**				
Gneiss	Gneiss (Nanga Parbat)	Whole sample	Lloyd et al. (2009)	EBSD	35.2	44.9	**19.9**	100								**5.90**				
Gneiss	Gneiss (Nanga Parbat; C-type)	C-type	Lloyd et al. (2009)	EBSD	32.3	30.6	**37.1**	100								**16.60**				
Gneiss	Gneiss (Nanga Parbat; S-type)	S-type	Lloyd et al. (2009)	EBSD	25.1	51.7	**23.2**	100								**11.60**				
Gneiss	Paragneiss	B-26	Long (1994)	Petrophysical	5	79.9	**15**	99.9	200	5.9233	4.5	6.4233	3.5	6.15	2	**8.10**	3.4633	1.25	**6.56**	Yes
Gneiss	Paragneiss	B-30	Long (1994)	Petrophysical	0.5	59.9	**37.1**	97.5	200	6.1133	1.5	6.3867	2.25	6.13	3.75	**4.37**				
Gneiss	Paragneiss	B-38	Long (1994)	Petrophysical	22.8	54.8	**13.4**	91	200	5.8467	2.25	6.5	4.25	6.5567	3.75	**11.45**				
Gneiss	Felsic gneiss	CD15	Watling (2017)	EBSD	35.6	22.4	**32.3**	90.3								**10.69**				
Gneiss	Felsic gneiss	CD19	Watling (2017)	EBSD	23.2	53.5	**23.4**	100.1								**9.87**				
Gneiss	Felsic gneiss	CD21	Watling (2017)	EBSD	25.1	38.1	**36.8**	100								**9.38**				
Gneiss	Felsic gneiss	CD22	Watling (2017)	EBSD	42.8	35.2	**22**	100								**13.42**				
Gneiss	Felsic gneiss	CD27	Watling (2017)	EBSD	54.6	13.5	**26.1**	94.2								**14.77**				
Mylonite	Mylonite (orthogneiss)	GFTZ-64	Burke (1991)	Petrophysical	28.1	62.9	**2.3**	93.3	300	6.141	1.7	6.058	2.6	6.25	1	**3.12**				
Mylonite	Mylonite (orthogneiss)	GFTZ-66	Burke (1991)	Petrophysical	27.7	60.1	**5.2**	93	300	6.042	2.4	6.275	2	6.25	1	**3.78**				
Mylonite	Mylonite (orthogneiss)	GFTZ-73	Burke (1991)	Petrophysical	29.4	66.4	**0.9**	96.7	300	6.154	1.3	6.245	2	6.099	0.3	**2.37**				
Mylonite	Mylonite (orthogneiss)	GFTZ-77	Burke (1991)	Petrophysical	28.7	62.6	**6**	97.3	300	6.244	1.3	6.254	1.3	6.341	0.7	**1.54**				
Mylonite	Mylonite (least deformed leucogneiss)	M13	Cirrincione et al. (2010)	Petrophysical	34.5	49.7	**12.5**	96.7	200-300	5.4383	10.5	5.3917	11.5	4.81	16	**12.26**	2.92		**23.52**	Yes
Mylonite	Mylonite (less deformed leucogneiss)	M8	Cirrincione et al. (2010)	Petrophysical	36.7	42.7	**15.6**	95	200-300	5.4097	11	5.4567	11	4.65	18	**15.96**	2.938		**22.91**	Yes
Mylonite	Mylonite (more deformed leucogneiss)	M3	Cirrincione et al. (2010)	Petrophysical	34.8	43.4	**19.4**	97.6	200-300	5.5303	9.9	5.5755	9.55	4.896	15.6	**12.98**	3.038		**19.60**	Yes
Mylonite	Mylonite (most deformed leucogneiss)	M4	Cirrincione et al. (2010)	Petrophysical	37.9	59.2	**1.7**	98.8	200-300	5.545	10.5	5.56	10	5.23	15	**6.12**	3.477		**6.17**	Yes
Mylonite	Granitic mylonite	MT-1	Ji et al. (1997)	Petrophysical	50	50	**0**	100	200	6.094	3.5	6.02	2.2	5.804	3.4	**4.87**				
Mylonite	Granitic mylonite	MT-5	Ji et al. (1997)	Petrophysical	50	50	**0**	100	200	5.88	2	5.86	2	5.832	2.7	**0.82**				
Mylonite	Felsic mylonite	GLG102	Ji et al. (2015)	EBSD	42.8	53.2	**3.4**	99.4								**3.30**				
Mylonite	Dioritic mylonite	GLG133	Ji et al. (2015)	Petrophysical	50	33	**15**	98	200	5.9195	3.7367	6.0757	3.0767	5.6525	2.8567	**7.22**	3.4792	4.6367	**6.11**	Yes
Mylonite	Dioritic mylonite	GLG133	Ji et al. (2015)	EBSD	50	33	**15**	98								**13.20**				